

# Modelling the Take-off Voltage of the Action Potential during Fast Pacing

Diandian Diana Chen<sup>1</sup>, Richard A Gray<sup>2</sup>, Flavio H Fenton<sup>1</sup>

<sup>1</sup>School of Physics, Georgia Institute of Technology, Atlanta, GA, United States

<sup>2</sup>US Food and Drug Administration, Silver Spring, MD, United States

## Abstract

*To date over 50 models for cardiac action potential have been developed, and while they vary widely in their complexity and the physiological characteristics that they reproduce, most fail to accurately replicate the takeoff potential during fast pacing and fibrillation. A specific aspect we focus is on the takeoff potential for an S2 stimulation following a steady S1 action potential. In microelectrodes and optical mapping experiment, the take-off voltage of an S2 action potential has been shown to be relatively high while most cardiac cell models do not reflect this feature, as the voltage needs to return close to the resting membrane potential before it can be reactivated. Since this difference can have great effects in electrical waves and their dynamics during tachycardia and fibrillation, we developed a framework that can be incorporated into the models to reproduce the experimentally observed higher take off potential.*

*Recovery of inactivation in the Sodium current is the key to the activation from an S2 stimulus. Therefore, we focused on the sodium inactivation gates  $h$  and  $j$ . We hypothesized that the  $j$  gate is the source of the low take off potential because it recovers during AP final repolarization. Our procedure is to model the dynamics of both gates via a single one with an adjustable time constant  $\tau$ . We model  $\tau$  with an asymmetric equation. Using this equation form, we can manipulate the width, height, and asymptotic values of  $\tau$ . The features that change the takeoff potential significantly are the midpoint and asymptotic value(s) of  $\tau$ . By shifting the midpoint value of  $\tau$  to a higher value, the takeoff potential increase, while rest of the sodium dynamics remains unaltered.*

## 1. Introduction

Fibrillation is one of the most dangerous cardiac

arrhythmias that has been shown to be driven by spiral waves of electrical activity[1][2]. When present in the ventricles it is deadly if not treated within minutes, when present in the atrium it is not immediately life threatening but affects the quality of life and can lead to strokes. Modeling of cardiac arrhythmias has become an important addition in the study of arrhythmias specially now with (I) a large number of models[3] developed and available to study the different mechanism in which arrhythmias can be induced, and (II) the increase in computer power by GPUs is beginning to allow large scale simulations of complex models in near real time without the need of supercomputers[4][5].

While there have been a large number of numerical simulations studies of fibrillation over the years, in all cases models have failed to show that during fibrillation the takeoff potential increases. Many studies with microelectrode (see for example figure 2 in Ref[6]) and optical mapping (see for example figure 1 in Ref[7]) have shown that during fibrillation the voltage of the takeoff potential (the minimum value of the voltage before an activation is elicited) increases during fibrillation and returns to normal (resting membrane potential) once the complex spatiotemporal dynamics has been terminated. Figure 1 shows an example of fibrillation in a canine right ventricle displaying the voltage signal from one point during fibrillation as a function of time. Top signal shows the numerical simulation and bottom signal the experimental trace, while the frequency of the arrhythmia is the same for both traces; it is clear that the voltage potential always returns to the resting membrane potential in the simulation but not in the experiment.

In this paper, we argue that the sodium current inactivation gate  $j$  may be underestimated in the time to re-open to activation on cell models, and thus we study modifications of the time constant and its effect on the takeoff of the action potential particularly during fast pacing.

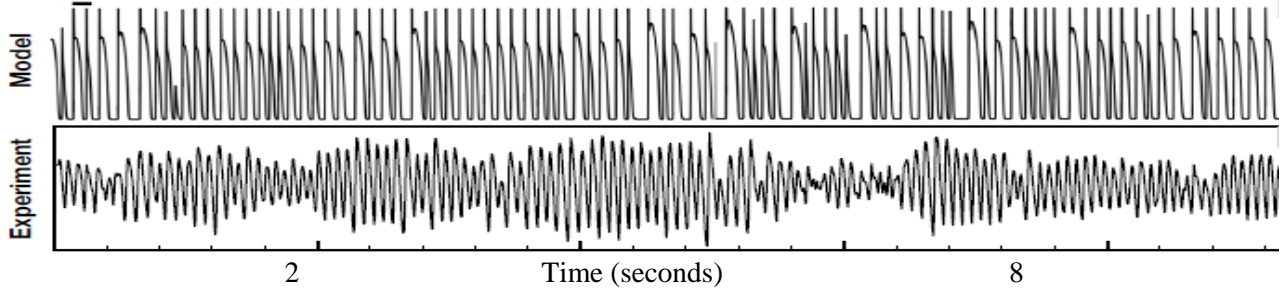


Figure 1. Action potential signal during fibrillation. (Top) simulation using a four variable model fitted to experimental data, (bottom) experimental data from a canine right ventricle during fibrillation using voltage optical mapping[8]. Notice that in the simulation the takeoff potential always goes back to the resting membrane potential.

## 2. Methods

### 2.1. Computational modeling

To study the takeoff potential and its dependence on the h and j gates, we chose to use two of the most common models used to study arrhythmias in computer simulations in two and three dimensions. The Beeler-Reuter (BR) [9] and the Luo-RudyI (LRI) [10] models. We also use in this study the Noble model[11] as it is a relatively simple model that can be used as a first test bed. However it is important to notice that the Noble model does not have any calcium dynamics and is for Purkinje cells/fibers, so not really adequate for fibrillation studies, but informative for fast pacing.

### 2.2. Numerical methods

All models were implemented in FORTRAN using an implicit Euler method to solve the propagation of AP along a 1D cable following the cable equation.

$$\frac{dV_m}{dt} = D \frac{\partial^2 V_m}{\partial x^2} - \frac{I_{ion}(V_m)}{C_m} + \frac{I_{stim}(x, t)}{C_m}$$

Where  $V_m$  is the membrane potential and  $D=0.001\text{cm}^2/\text{msec}$  is the diffusion along the cable consisting of 500 elements with a spatial discretization of  $dx=0.025\text{cm}$  and an integration time of  $dt=0.01\text{ms}$ .  $I_{stim}$  is the stimulation current applied at a given period to the first 10 elements of the cable and  $I_{ion}$  represents the currents for the Noble, BR and LR-I models.

### 2.3. Asymmetric time constant

As stated in the introduction, we hypothesized that the low take off potential of cardiac simulations is controlled by the voltage dependent time constant of j. In addition, the equations for its time constant are complex. We therefore choose to simplify the equations for the time constants by the following functions.

$$\tau_i^- = \tau_0^- [\delta^- - \tanh(a^-(V_m - V_i^-))]/2$$

$$\tau_i^+ = \tau_0^+ [\delta^+ + \tanh(a^+(V_m - V_i^+))]/2$$

Where  $\tau_i^-$  is used for  $V_m > V_{peak}$  and  $\tau_i^+$  for  $V_m \leq V_{peak}$ .  $V_{peak}$  is the point for the maximum of the function,  $\tau_0, \delta, V_i$  and  $a$  represent the amplitude, asymptote, inflection and steepness respectively. Figure 2 shows  $\tau_j$  for the Noble and BR models and then respectively fitted  $\tau_i^-$  and  $\tau_i^+$  but shifted to a higher voltage.

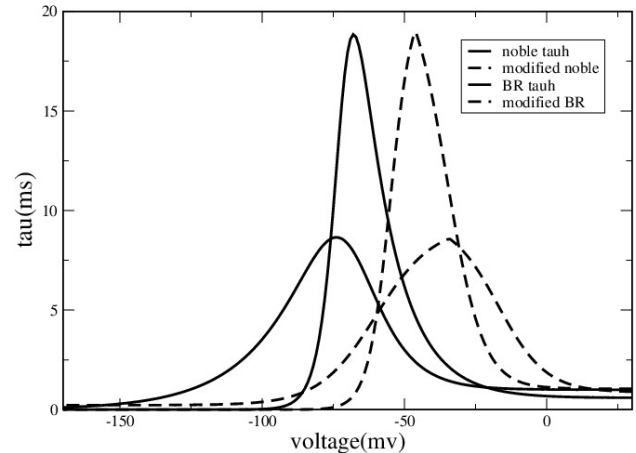


Figure 2.  $\tau_h$  for Noble and  $\tau_h$  BR model (higher amplitude) and shifted  $\tau_i^-$  and  $\tau_i^+$  for each model.

Value parameters are [9,1.5, 0.05,-60, 8.7, 1.2, .06, 17] for Noble fit and [21,1,0.13,-55 , 21, 1.1, 0.08,-35] for Beeler-Reuter fit.

By adjusting the parameters of  $\tau_i^-$  and  $\tau_i^+$ , we are able to adjust the shape and height of the time constant to specific values as shown in figure 2. Changing a single parameter on the time constant does not result in a single isolated effect on the take of potential, however shifting the peak to higher voltages has the largest effect.

### 3. Results

The main goal of modifying the time constant is to increase the takeoff potential to match experimental values. Before the shape and position of the time constant is varied, we have checked that substituting the fitted  $\tau_i^-$  and  $\tau_i^+$  does not change the dynamics of the models.

#### 3.1. 0D simulations

To show the effect of  $\tau_i^-$  and  $\tau_i^+$ , we plot the sodium current  $I_{Na}$  versus s2 duration in 0D (single cells). Figure 3 shows the result of shifting the fitted  $\tau_i^-$  and  $\tau_i^+$  midpoints to higher voltage values on the LR model. This shift results in  $I_{Na}$  being excited earlier, and thus can produce activations during phase III of the action potential. This in turn can lead to higher take-off potentials. The most successful adjustments are when the midpoint  $V_{peak}$  is shifted to higher potentials, in Fig. 3 from -66 to -60,-51, and -36 mV.

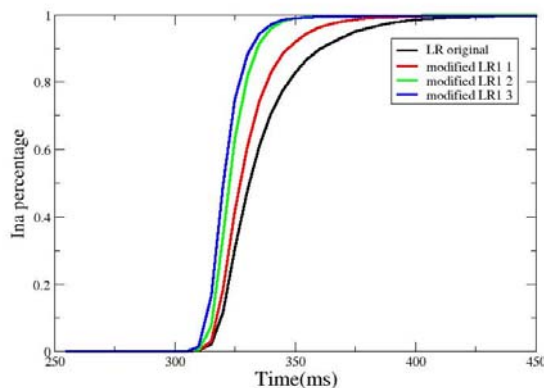


Figure 3.  $I_{Na}$  as a function of S2 activation times, showing how in single cell, modifying  $\tau_i^-$  and  $\tau_i^+$  can increase sodium current at shorter and shorter

activations resulting in smaller diastolic intervals.

#### 3.2 1 D simulations

Simulations in 1D were carried in cables of 500 cell elements for Beeler Reuter and 100 cell elements for Noble. Stimulation was produced on the first 10 elements and measurements of action potentials were performed at cells 30, 40 and 99. To enhance the effect of the time constant we eliminated for the BR and LR models the slowest gate j. Effectively, we reduced the inactivation gates to one gate, h. Then we replaced the time constant of the h gate with the two piecewise equations introduced above.

Shown below is an example of increased take off potential in the Noble model with its normal  $\tau_h$  (Fig. 4) and with the fitted  $\tau_i^-$  and  $\tau_i^+$ , shifted by 40 mV for an S1-S2 pacing protocol. S1 indicates a first stimulus and S2 is a second stimulus that is applied at shorter and shorter periods until just before conduction block is produced. Figure 5 Shows similar dynamics but for the BR model before and after the shift of the time constant. For this case we have also increased slightly the time for which the m gate remains open during the AP, all resulting in an elevated take-off potential of about 14 mV.

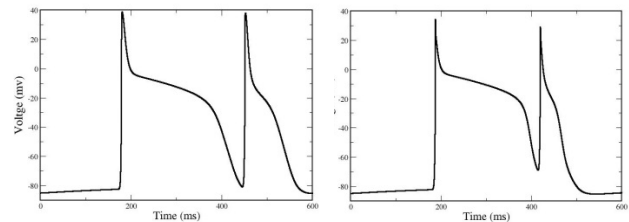


Figure 4. Action potentials (AP) using the Noble model for an S1 and S2<sub>minimum</sub>. Right, for the original model and left for the modified model showing an increase of 11.5 mV in the takeoff potential.

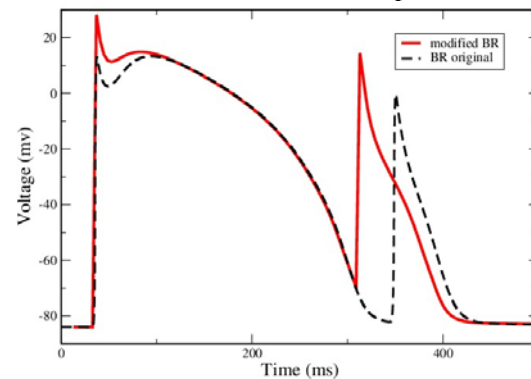


Figure 5. AP from BR model original (dash lines)

and modified (solid lines) showing a shorter diastolic interval and elevated take off potential of -70 mV

To demonstrate that take off potential can be increased during simulated fibrillation as in figure 1 (experimental) we pace the Noble model at a 500ms cycle length and then abruptly increased it to 60ms for about 5 pulses where the takeoff potential is elevated by 14 mV.

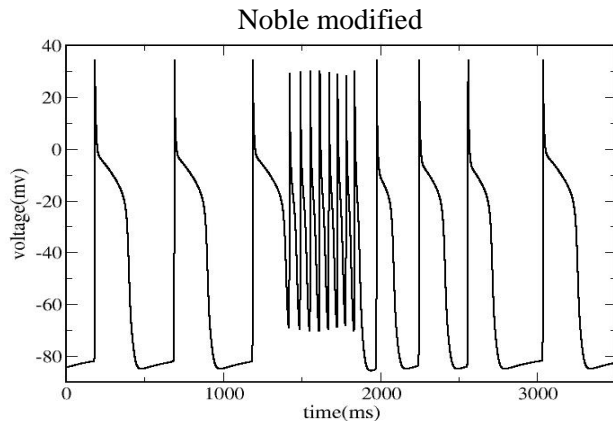


Figure 6. To simulate fibrillation in 1D cable, the Noble model is paced at a very high cycle length during which time the takeoff potential is elevated.

#### 4. Limitations

The change of the time constant  $\tau_i$  can affect the beginning of the upstroke of the action potential and thus may affect the shape of the action potential. Particularly for models that have either very strong L-type Calcium current or relatively low sodium current[12]. It is possible that other modifications to the sodium current including changes in its maximum conductance could help in recovering the shape lost in those models. This study did not present any results in 2D simulations and while take off potential increased during fast S2 activations, its effect during fibrillation needs to be verified.

#### Acknowledgements

This work has been supported by NSF (FDA scholars in residence program) grant #1347015.

#### References

[1] Davidenko JM, Pertsov AV, Salomonsz R, Baxter W, Jalife J. Stationary and drifting spiral waves of

excitation in isolated cardiac muscle. *Nature* 1992;355:349–351.

- [2] Cherry EM, Fenton FH. Visualization of spiral and scroll waves in simulated and experimental cardiac tissue. *New J. Phys.* 2008; 10: 125016.
- [3] Fenton FH, Cherry EM. Models of cardiac cell. *Scholarpedia* 2008;3:1868.
- [4] Vigmond EJ, Boyle PM, Leon L, Plank G. Near-real-time simulations of bioelectric activity in small mammalian hearts using graphical processing units. *Conf Proc IEEE Eng Med Biol Soc* 2009;3290–3293.
- [5] Bartocci E, Cherry EM, Glimm J, Grosu R, Smolka SA, Fenton FH. Toward real-time simulation of cardiac dynamics. *CMSB 2011: Proceedings of the 9th International Conference on Computational Methods in Systems Biology, Paris, France, 2011*; 103–110.
- [6] Zhou X, Guse P, Wolf PD, Rollins DL, Smith DM, Ideker DE. Existence of both fast and slow channel activity during the early stages of ventricular fibrillation. *Circ Res* 1992; 70 :773–786.
- [7] Fenton FH, Luther S, Cherry EM, Otani NF, Krinsky V, Pumir A, Bodenschatz E, Gilmour Jr RF.. Termination of atrial fibrillation using pulsed low-energy far-field stimulation. *Circulation* 2009; 120 : 467–476.
- [8] Filippi S, Gizzi A, Cherubini C, Luther S, Fenton FH. Mechanistic insights into hypothermic ventricular fibrillation: the role of temperature and tissue size. *Europace* 2014; 16 : 424–434.
- [9] Beeler GW, Reuter H. Reconstruction of the action potential of ventricular myocardial fibres. *J Physiol* 1977; 268: 177–210.
- [10] Luo CH, Rudy Y. A model of the ventricular cardiac action potential. Depolarization, repolarization, and their interaction. *Circ Res* 1991; 68:1501–1526.
- [11] Noble D. A modification of the Hodgkin–Huxley equations applicable to Purkinje fibre action and pace-maker potentials. *J Physiol* 1962; 160:317–352.
- [12] Cherry EM, Fenton FH. A tale of two dogs: analyzing two models of canine ventricular electrophysiology. *Am J Physiol* 2007; 292:43-55.

Address for correspondence:

Diandian Diana Chen  
School of Physics, Georgia Institute of Technology. 837  
State Street, Atlanta, GA 30332.  
dchen87@gatech.edu